The magnetosheaths of the outer planets

John D. Richardson *

Centre for Space Research, Massachusetts Institute of Tech., Cambridge, MA 02139, USA

Abstract

This paper provides a review of past work on the magnetosheaths of the outer planets and also provides the most complete look to date at the plasma parameters in these magnetosheaths. We find that proton distributions in the magnetosheaths of Jupiter, Saturn, and Neptune (but not Uranus) are well represented by two Maxwellians with the same velocity but different temperatures. The hot proton component comprises about 40% of the total density and has a temperature about six times that of the cold protons. The Jovian magnetosheath shows significant motion, with sunward flow not uncommon when the magnetosheath region moves outwards, probably due to changes in solar wind pressure. Gas dynamic models of the boundaries show that the magnetospheres of Jupiter and Saturn are flattened at the poles. Deviations from the predictions of gas dynamics are observed, both because of time-dependent effects and systematic effects such as encounters with the plasma depletion layer and plasma mantle, both of which are MHD effects. Mirror mode waves are ubiquitous in the magnetosheaths, but other waves and oscillations are also observed, including one so far unique to Uranus which may occur downstream of parallel shocks. © 2002 Elsevier Science Ltd. All rights reserved.

1. Introduction

The magnetosheaths of the outer planets have similarities to that of Earth but also significant differences. The magnetosheath consists of solar wind which passes through the bow shock, becomes subsonic, and then flows around the planetary obstacle, the magnetosphere. The attributes which are unique to the outer planets are that the obstacle sizes are much larger than Earth's magnetosheath, the obstacle shapes and magnetic field configurations differ, and the plasma and magnetic field are much more tenuous giving longer scale lengths. This paper is both a review and presentation of un-published work. We discuss various aspects of the magnetosheaths of the outer planets: ion distributions, comparisons of magnetosheath shapes and ion parameters to gas dynamic models, and waves both within and on the inner boundary of the magnetosheath.

The outer planets are much larger than Earth, have surface magnetic fields which are comparable to or larger than that of Earth, and are embedded in a much more tenuous solar wind plasma than is Earth. Important parameters for describing the interaction of the supersonic solar wind with an obstacle such as a planetary magnetosphere are the obstacle size and shape, the solar wind Mach number, and the plasma beta. The solar wind density N decreases as R^{-2}, the radial and tangential components of the magnetic field B_R and B_T as R^{-2} and R^{-1}, respectively, and the ion temperature T_I as $R^{-0.5}$ (Richardson et al., 1995). The electron temperature beyond about 5 AU was too cold for Voyager to measure, but is thought to decrease at a similar rate as the ions. The fast mode, or magnetosonic, Mach number M_{MS} is defined as $V_{SW}/\sqrt{V_A^2 + C_S^2}$ where V_{SW} is the solar wind speed, the Alfven speed $V_A \alpha B/\sqrt{N}$, and the sound speed $C_S \alpha T_e$, where T_e is the electron temperature. As the solar wind moves outward, M_{MS} will decrease due to the decrease of B_R and T_e. The plasma beta, the ratio of plasma to magnetic pressure $\beta \alpha N T_I/B^2$, decreases as T decreases in the outer heliosphere. The solar wind is not a uniform medium; in particular density variations are large and remain so in the outer heliosphere. Table 1 shows the distances of the four outer planets in AU, the range of magnetopause sizes encountered by the Voyager spacecraft at each planet, the range of Mach number and plasma beta upstream of the observed shocks at each planet, the average hot N_H component and total N_T densities in the dayside magnetosheath, the ratio N_H/N_T in the magnetosheath, and the ratio of hot (T_H) to cold (T_C) ion temperature in the magnetosheath. The last four rows are discussed below.

* Tel.: +1-617-253-6112; fax: +1-617-253-0861.

E-mail address: jdr@space.mit.edu (J.D. Richardson).

Table 1

	Jupiter	Saturn	Uranus	Neptune
Distance from Sun (AU)	5	10	19	30
Magnetopause Standoff Distance (R_p)	45–70	19–23	18	26
Observed M_{MS}	3–18	4–11	17	8.8
Observed β	0.2–6	0.1–4	5	0.23
Mean N_H	0.51	0.12	0	0.0053
Mean N_T	1.5	0.36	0.23	0.011
Mean N_H/N_T	0.39	0.38	0	0.48
Mean T_H/T_C	6.3	11.4	0	13.0

2. Ion distributions

Ion distributions in Earth's magnetosheath often have a high-energy tail which generally contains less than 10% of the total density and usually occurs near the shock (Howe, 1970; Hundhausen et al., 1969; Wolfe and McKibben, 1968; Montgomery et al., 1970). Zastenker et al. (1994) found the higher-energy proton component comprises 10–20% of the total proton density, but that the higher-energy alpha (He^{++}) component comprised 25–50% of the total alpha density. Sanders et al. (1978, 1981) and Peterson et al. (1979) reported observations where the density of the hot component was comparable to or greater than that of the cold component, but these distributions seem rare at Earth. The hot component of the ions is thought to be comprised of ions which are reflected at their first encounter with the bow shock and gain additional energy as they pass through on their second attempt (Sckopke et al., 1983). A combination of observations and shock modeling has predicted that the percentage of hot ions asymptotically approaches 20% as the Mach number of the upstream flow increases (Fuselier and Schmidt, 1994).

Observations of the outer planets have been made by Pioneer 10 (Jupiter), Pioneer 11 (Jupiter and Saturn), Voyager 1 (Jupiter and Saturn), Voyager 2 (Jupiter, Saturn, Uranus, and Neptune), Ulysses (Jupiter) and Galileo (Jupiter). Pioneer 10 and 11 observations of the Jovian magnetosheath found that many of the distributions were Maxwellian, but some had non-Maxwellian characteristics with enhancements at low or high energy (Mihalov et al., 1976). Near the shock two-temperature distributions were reported with characteristics of both the unperturbed solar wind and magnetosheath plasma (temperatures of about 3 and 280 eV, respectively), but these spectra probably indicate incomplete shock crossings rather than shock-produced distributions.

Richardson (1987) surveyed the inbound magnetosheath distributions observed by Voyagers 1 and 2 at Jupiter and Saturn, looking at roughly one point each hour. The distributions throughout the dayside magnetosheath were well represented by a two-temperature proton distribution. The density of the hot proton population comprised 20–50% of the total density and the temperature of the hot component is

6–10 times that of the cold component. Phillips et al. (1993) reported that similar distributions were observed by Ulysses in the dawn and dusk flanks of the Jovian magnetosheath from the magnetopause to the bow shock. The Voyager 2 pass through the dayside Uranian magnetosheath did not find two-temperature distributions; the data were well represented by single Maxwellians (Richardson, 1987). Neptune was similar to Jupiter and Saturn; the dayside magnetosheath distributions were best modeled using two proton Maxwellians (Szabo and Lepping, 1995). Although Galileo has made many crossings of the Jovian magnetosheath, these data are not yet in the literature.

The ion distributions are important for understanding the physics of planetary bow shocks and interplanetary shocks in general since the hot component consists of ions initially reflected at the shock, and hence should be carried in the total mass flux budget of the shocks. The ion distributions are also important for understanding wave growth and damping. Taking advantage of enhanced computing capacity, we have reanalyzed all the Voyager 1 and 2 inbound (dayside) magnetosheath data at Jupiter and Saturn. We fit these spectra using the same assumptions and method as Richardson (1987); plasma distributions are assumed to consist of two proton convected isotropic Maxwellians with the same bulk velocity but different number densities and thermal speeds. The Voyager plasma experiment (PLS) cannot discriminate between protons and alphas in the magnetosheath, so the 3–5% (on average) of the number density in the alpha component makes a contribution to the hot proton component, but the effect of the alphas on the results presented here should be minimal.

Voyagers 1 and 2 are three-axis stabilized spacecraft. The PLS experiment consists of four modulated-grid Faraday cups which measure ion current in the energy-per-charge range of 10–5950 eV (see Bridge et al., 1977). The instrument has a high-energy resolution (M) mode ($\Delta E/E = 3.6\%$) and a low-energy resolution (L) mode ($\Delta E/E = 29\%$), both of which are used in this analysis. Three cups (A–C) are optimized for solar wind detection and thus look sunward into the nominal magnetosheath flow. The fourth cup (D) looks at right angles to this direction but still detects ion fluxes in the magnetosheath since the plasma is subsonic. Currents are measured simultaneously in all four cups, with a new set of L mode spectra obtained every 96 s and a new set of M mode spectra every 192 s.

Fig. 1 shows a typical fit of two Maxwellians with different temperatures to a set of M mode spectra from the Jovian magnetosheath. The histogram shows the measured current in femtoamperes (10^{-15} A) plotted versus a logarithmic energy scale. The best fit to the data using two proton convected isotropic Maxwellians with the same bulk velocity is shown by the bold curve with x's; the other two curves show the contributions to the total simulated current from each proton component. Similar fits are performed on all the spectra from the Jovian and Saturnian magnetosheaths except for a few contaminated by noise.
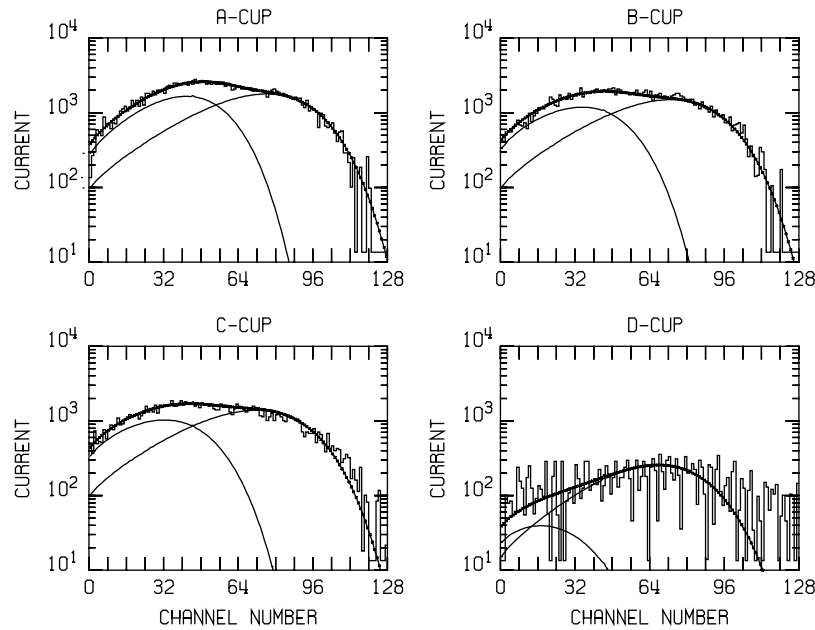
Fig. 1. A typical set of spectra from the Jovian magnetosheath. These spectra were obtained by Voyager 2 about 70 Jovian radii from the planet. The data are shown by the histograms. The best fit to the data (bold line) contains contributions from two Maxwellians (light lines). The two-temperature proton distribution gives the best fit with $(V_R, V_T, V_N) = (114, 87, 1)$ km/s, $n_{COLD} = 0.68$ cm^{-3}, $T_{COLD} = 100$ eV, $n_{HOT} = 0.79$ cm^{-3}, and $T_{HOT} = 598$ eV.

For all but 4–5 sets of spectra, the data were best fit using two Maxwellians. The only spectra for which this distribution did not work were at Jupiter when the magnetosheath plasma was flowing outward (sunward) so rapidly that the cold component could not be detected by the Faraday cups, so that only the hot Maxwellian was observed.

For a two Maxwellian distribution, the important parameters are the density and temperature ratios of the two components. Figs. 2 and 3 show these values in Jupiter's and Saturn's magnetosheaths. The Voyager spacecraft made eight complete passes through the dayside magnetosheath of these planets, from bow shock to magnetopause, three each by Voyagers 1 and 2 at Jupiter, and one each by Voyagers 1 and 2 at Saturn (one each of the Voyager 1 and 2 Jovian crossings were due to the expansion of the magnetosheath past the spacecraft; numerous other entrances into the magnetosheath occurred and are shown later). For ease of comparison of these passes, the x-axis on the plots goes from the bow shock (left) to magnetopause (right); thus the point spacing varies depending on the length of the crossing. The bow shock locations, magnetopause locations and upstream conditions for each crossing are shown in each panel. Mach numbers range from 9 to 19 and plasma β's from 0.4 to 11. The percentage of density in the hot component ranges from 10% to 50%; this percentage can be quite variable (third and fourth panels) or steady (sixth panel) across the magnetosheath. The average percentage is about 40%. The ratio of the hot to cold temperature varies from 4 to 12. This ratio also varies with time, presumably due

to changes in the shock, not evolution of the propagating distributions as demonstrated below. For the Neptune data (not shown), the average percentage of hot protons is 48% and the ratio of the hot to cold temperature components is 13, considerably larger than at Jupiter or Saturn.

Figs. 4 and 5 show plasma and magnetic field parameters as a function of time in the Jovian inbound magnetosheath. All inbound magnetosheath data are shown as opposed to Figs. 2 and 3 which show only complete magnetosheath crossings. The left boundary is the first bow shock crossing and the right boundary the last inbound magnetopause crossing. The other bow shock and magnetopause crossings are shown by the dashed lines, with the regions between labeled as either magnetosphere (MSP) or SW. The ratio of the hot to total density varies from 0.15 to 0.7. The Voyager 2 data on day 185, in particular, seem to show a bimodal distribution, with the density ratio quantized at either 0.3 or 0.5. Weaker evidence of a two-state system is seen in the last magnetosheath crossing in the Voyager 1 data. The hot and cold temperature profiles track very well; temperature ratios T_H/T_C vary from 4 to over 10. The density ratio is generally positively correlated with the temperature ratio, although this correlation does not always hold. Thus, when more energy needs to be dissipated at the shock, this energy ends up both as a higher percentage of hot ions and a hotter temperature of hot ions.

We look for dependences of the density and temperature ratios of the two proton distributions on the plasma and magnetic field parameters. The only parameter upon which the density and temperature ratios seem to depend is the
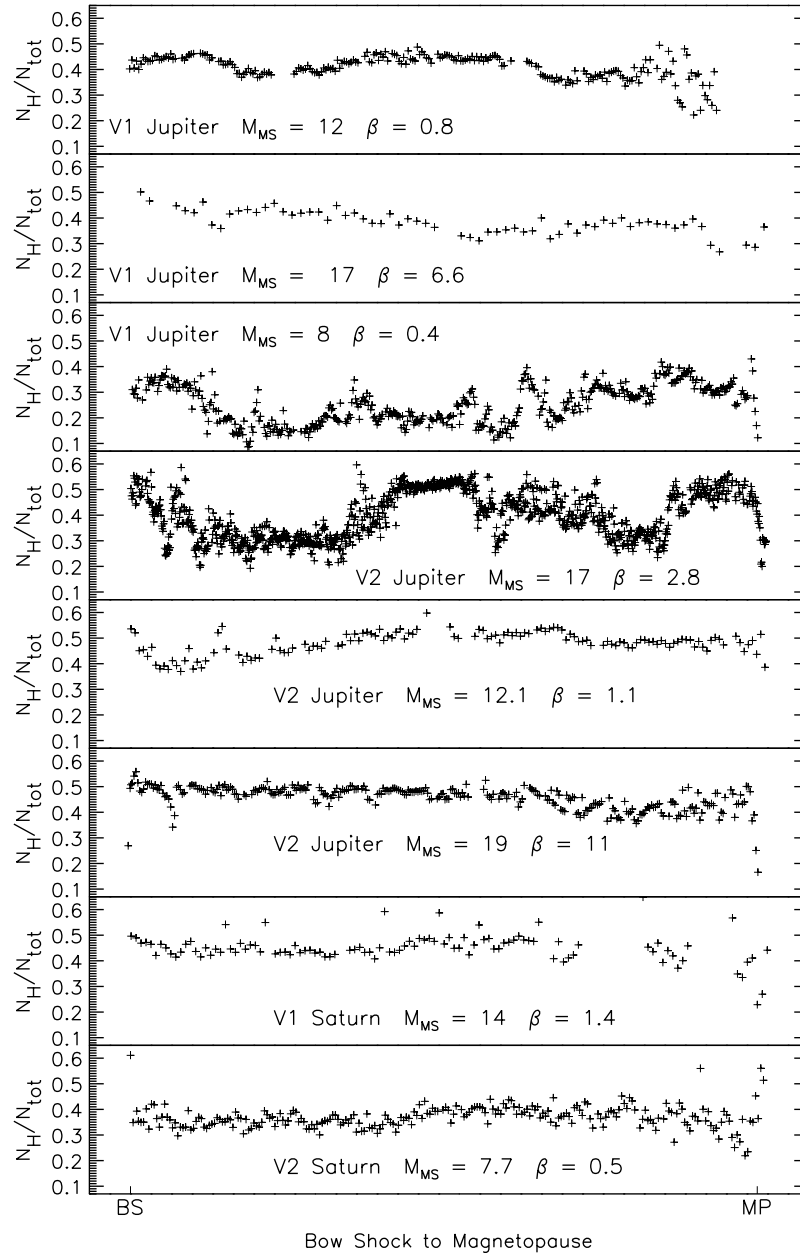
Fig. 2. Ratio of hot proton density to total proton density for the eight complete passes through the magnetosheaths of Jupiter and Saturn. The Mach numbers and plasma β's upstream of each shock crossing are shown. The density of the data points depends on the duration of the magnetosheath crossing.

radial component of speed. Higher speeds correspond to both a higher percentage of hot ion density and a higher T_H/T_C ratio. Since higher speeds in the solar wind generally correspond to higher speeds in the magnetosheath, this suggests that the additional energy in the solar wind ends up in the hot component.

We note that the percentages of hot ions observed in these magnetosheaths are significantly larger than the 20% limit found for Earth's magnetosheath by Fuselier and Schmidt (1994). Plasma densities and magnetic field strengths are much smaller and shock scales much larger than at Earth

which may allow for this discrepancy. If we look at the percentage of hot ions in the magnetosheath near the bow shock crossings, the percentage may have a dependence on a Mach number, with percentages near 50% when the Mach number is over 13 and under 40% for Mach numbers under 9. The distance, M_{MS}, and β for each shock crossing are shown in Table 2; all the shocks are quasi-perpendicular. No dependence of the temperature ratio on either the Mach number or β is apparent.

Figs. 6 and 7 show the same parameters in the Saturnian magnetosheath. The magnetosheath passes are shorter since
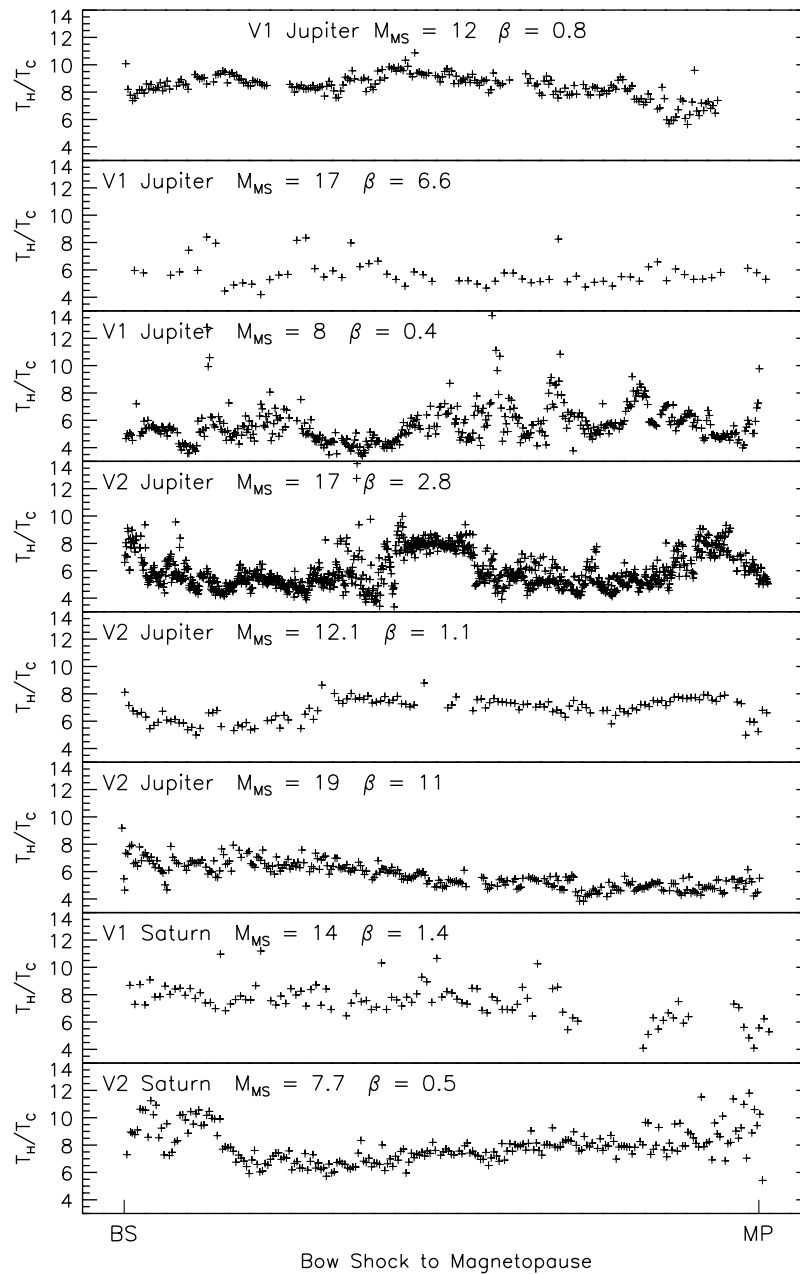
Fig. 3. Ratio of the hot/cold temperatures of the two proton components. The Mach numbers and plasma β's upstream of each shock crossing are shown.

the magnetosphere is much smaller, but, in general, the same relationships hold as for Jupiter. One difference is the much larger hot component temperature observed by Voyager 2 in its first excursion into the magnetosheath, with the hot temperature near 2 keV giving temperature ratios T_H/T_C of 15–30.

3. Plasma parameters

The radial speeds observed in the magnetosheath range from 250 km/s planetward to over 200 km/s sunward. These speed extremes result from superposition of changes in the solar wind pressure and flow around the object. The multiple crossing of the bow shock and magnetopause arise from the solar wind pressure changes and these effect the radial speeds. For example, the magnetosheath crossing by Voyager 1 starting near day 61.3 occurred when a large increase in solar wind pressure pushed the whole magnetosheath region past Voyager 1 so that the spacecraft went from the magnetosphere to the solar wind in 1.9 h. The inward speed in this crossing was as large as 220 km/s. In contrast, the last crossing of the magnetosheath by Voyager 1 (day 61.54–62.1) had large regions of negative (outward) flow
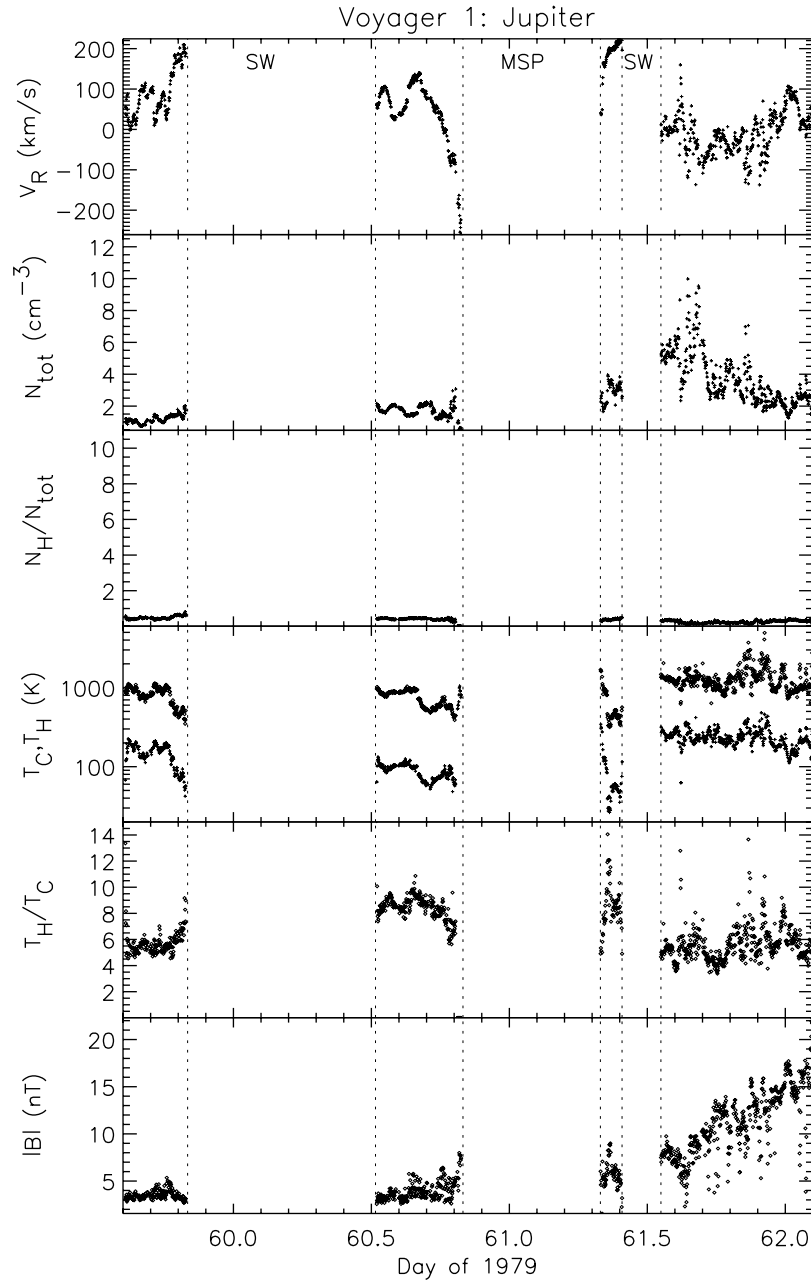
Fig. 4. The inbound magnetosheath data from Voyager 1 at Jupiter. Periods where Voyager 1 was in the solar wind and magnetosphere are labeled SW and MSP, respectively. From top to bottom are shown the radial speed, total proton density, ratio of the hot density component to the total density, hot and cold proton temperatures, ratio of hot to cold proton temperature, and magnitude of the magnetic field.

resulting from a decrease in solar wind pressure and expansion of the magnetosphere. Siscoe et al. (1980) first reported that Voyager 1 observations suggested sunward flow in Jupiter's magnetosheath and Richardson (1987) confirmed these results finding sunward speeds of up to 200 km/s. Sunward flow occurs when the solar wind dynamic pressure decreases and the expanding magnetosphere drives plasma in the magnetosheath ahead of it. Siscoe et al. (1980) show that a new stagnation point is created in the magnetosheath,

as shown in Fig. 8. They calculate the distance at which the stagnation point forms as a function of the ratio between the sunward speed and solar wind speed; although we do not have simultaneous solar wind measurements, for the largest sunward speeds (200 km/s) a large, > 50%, portion of the magnetosheath flow must be sunward. These large regions of sunward flow are so far unique to Jupiter. One reason they exist at Jupiter is that, compared to Earth, the magnetosphere of Jupiter is highly compressive with the
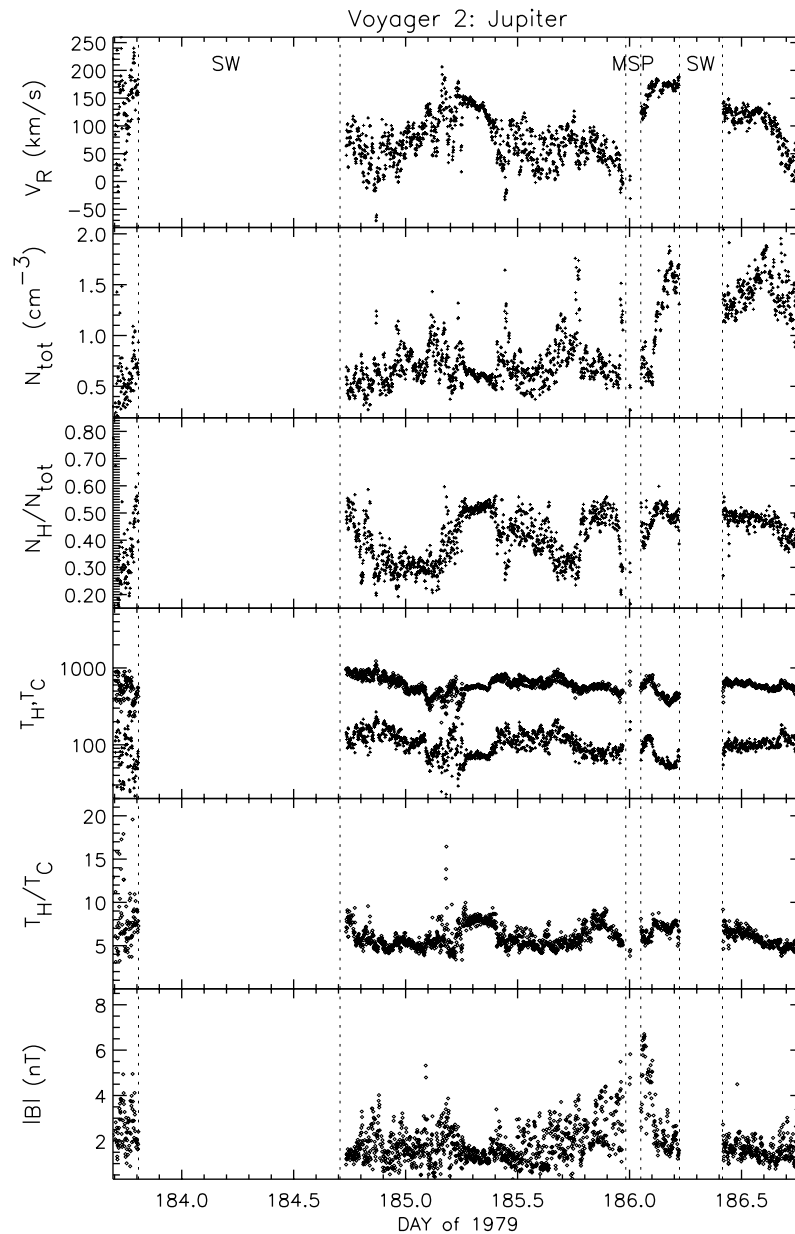
Fig. 5. The inbound magnetosheath data from Voyager 2 at Jupiter. Periods where Voyager 1 was in the solar wind and magnetosphere are labeled SW and MSP, respectively. From top to bottom are shown the radial speed, total proton density, ratio of the hot density component to the total density, hot and cold proton temperatures, ratio of hot to cold proton temperature, and magnitude of the magnetic field.

magnetopause standoff distance proportional to the solar wind pressure to the $-1/3$ power (at Earth it is proportional to the solar wind pressure to the $-1/6$ power). This greater compressibility is a result of the plasma pressure inside the magnetosphere providing a substantial amount of the internal pressure to hold off the solar wind.

The magnetosheath densities are generally lower in magnetosheath farther from the planet; this result is largely a selection effect as the solar wind pressure depends mostly on the density, so the spacecraft are in the magnetosheath far from the planet only when the solar wind density is low. Near the magnetopause crossings densities are sometimes observed to decrease, particularly near the last inbound crossings of Voyager 2 at Saturn and Jupiter. The magnetic field magnitude also increases in these decreased density regions. These are signatures of entry into the plasma depletion layer (PDL), similar to signatures seen at Earth. In the PDL, draping of the magnetic field around the magnetosphere causes the field magnitude to increase and the increased magnetic pressure causes the plasma to move along the magnetic field out of this high-pressure region (Zwan and Wolf, 1976).

Table 2
Distance of shock from the planet and solar wind Mach numbers and β's for each dayside bow shock

V1 Jupiter			V2 Jupiter		
R_J	M_{MS}	β	R_J	M_{MS}	β
85.6	8.7	0.26	98.6	3.9	0.18
82.3	11.8	0.72	97.3	12.1	0.71
71.7	11.6	0.79	86.6	17.0	2.8
57.8	17.6	6.6	68.8	12.1	1.1
55.7	8.1	0.40	66.5	19.2	11.0
V1 Saturn			**V2 Saturn**		
R_S	M_{MS}	β	R_S	M_{MS}	β
26.1	14.0	1.4	23.6	7.7	0.54
			V2 Uranus		
			R_U	M_{MS}	β
			23.6	17.	3.6
			V2 Neptune		
			R_N	M_{MS}	β
			34.8	8.8	0.23

4. Gas dynamic model comparisons

The gas dynamic models developed by Spreiter and Stahara have been applied to the outer planets in a number of studies. Slavin et al. (1985) compared the locations of the bow shocks predicted by gas dynamic theory with those observed (using the observed magnetopause location for the obstacle size). They found that for both Jupiter and Saturn the gas dynamic model predicted a bow shock location significantly further upstream from the magnetopause than observed. They hypothesized that the magnetopauses of these planets could be flattened at the poles, since the energetic particles which provide internal pressure are confined near the equator. Stahara et al. (1989) adapted their gas dynamic model to test this hypothesis, allowing the ratio of the semi-major to semi-minor axis (a/b) to be adjustable. They then varied the ratio of the equatorial/polar (a/b) radii until they were able to match the data. Fig. 9 shows they obtain a good fit to the bow shock position for Jupiter with $a/b = 1.75$. For Saturn (not shown) they find $a/b = 1.25$. Stahara et al. (1989) report that the observed bow shock at Saturn is still more highly flared than predicted, but with few data points available this may not be a real effect. This result, that the magnetosphere of Jupiter and Saturn are flattened at the poles, was a major accomplishment for gas dynamic theory.

As part of the above work, Stahara et al. (1989) modified their calculation of magnetosheath parameters and published maps of magnetosheath properties in the Jovian ecliptic and meridional planes. We use the results to compare with the observed values in the magnetosheath in Fig. 10. Data from the three complete magnetosheath crossings by each Voyager at Jupiter are shown in separate panels by the points and the model values are shown by the lines. The model assumes

the ratio $a/b = 1.75$, the Mach number $M = 10$, and the ratio of specific heats $\gamma = 2$; it of course assumes steady state which is not valid. We plot magnetosheath values normalized by the upstream solar wind values. The measured number densities plotted are the total density and the temperature the weighted mean temperature. For all profiles, speed, density, and temperature, the profiles show significant differences in both shape and absolute value. Some of this variation is due to the different upstream conditions (although the parameters are normalized to upstream parameters, Mach numbers, β's, and γ's can vary). The general shape of the speed profile predicted by the gas dynamic model matches the observed speed profile quite well, although time-dependent deviations from the model are apparent. The density profile for Voyager 2 at Jupiter matches the model shape fairly well, but for Voyager 1 through the Jovian magnetosheath the data show a decrease in density across the magnetosheath while the model predicts an increase. Near the magnetopause there is evidence for a PDL, which is not a gas dynamic effect and thus not predicted by the model. The magnitudes of the observed densities are consistently higher than those predicted; we do not understand this discrepancy. The gas dynamic model treats the solar wind as a one-fluid model, and thus does not, in general, get the ion temperature magnitude correct. The model predicts a flat temperature profile and this prediction is fairly consistent with observations.

Fig. 11 shows a similar plot showing the two complete passes through Saturn's magnetosheath compared to gas dynamic predictions. Since Stahara et al. (1989) did not publish their model results for the $a/b = 1.25$ case appropriate for Saturn, we compare to the $a/b = 1.75$ case. The two passes are quite similar. The speed decreases across the magnetosheath, although somewhat less than the gas dynamic prediction. The observed density profiles decrease slightly from the bow shock toward the magnetopause, while the model predicts an increase. Near the magnetopause clear evidence of the PDL is seen in both profiles. Voyager 1 observed temperatures about 30% higher than those observed by Voyager 2, and both were higher than the gas dynamic value.

The gas dynamic model was used by Richardson et al. (1994) to model the magnetosheath at Neptune. As Spreiter and Stahara (1994) point out, with a solar wind density of 0.005 cm^{-3} this may be the lowest density medium to which continuum fluid theory has been applied. Solar wind parameters upstream of the bow shock were used to determine plasma values in the magnetosheath along the Voyager 2 trajectory. On the dayside, a reasonable fit to the data was found. The most important results came from fitting the data on the night side (Zhang et al., 1990). Fig. 12 shows plasma and magnetic field data from Neptune's outbound magnetosheath (jagged lines) and gas dynamic predictions (smooth curves). In general, the agreement is good. One goal of comparison of data with gas dynamic theory is to see where the theory breaks down. Comparison with the gas dynamic model shows regions where the density and radial velocity are lower than predicted and the magnetic field
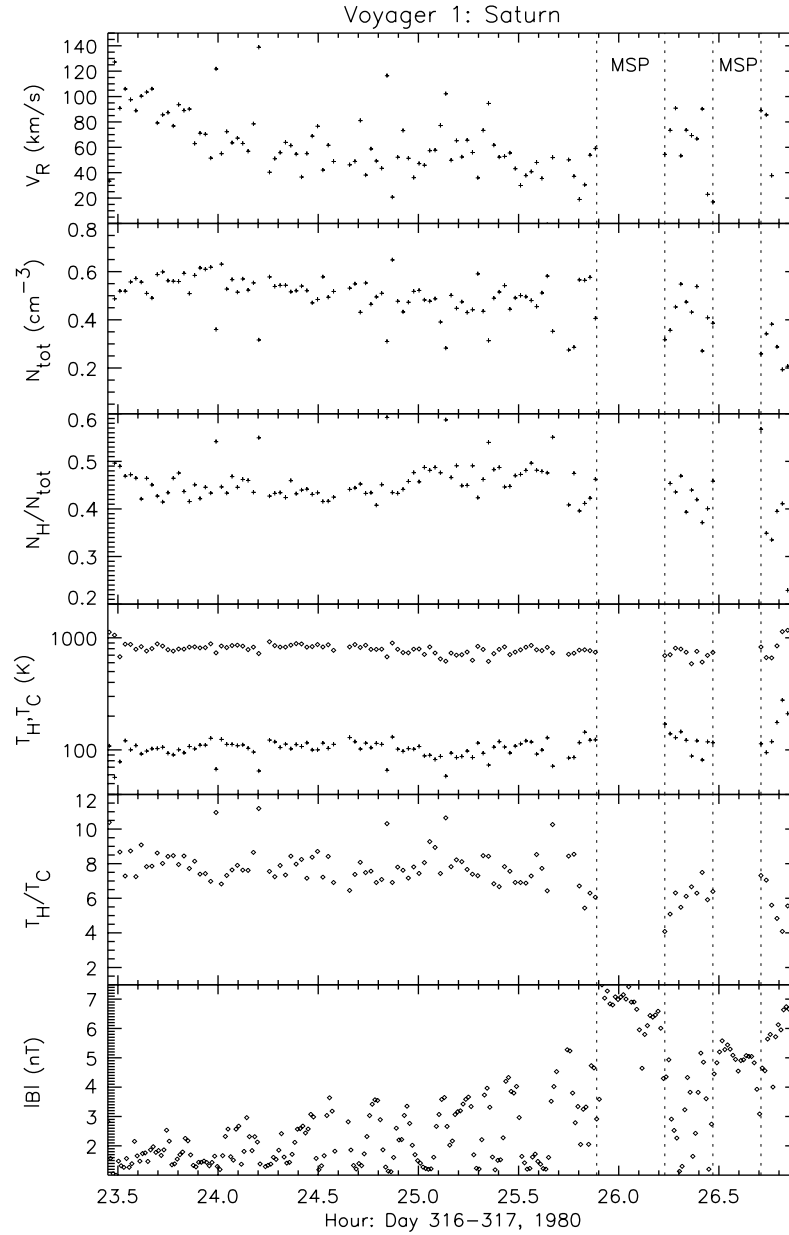
Fig. 6. The inbound magnetosheath data from Voyager 1 at Saturn. Periods where Voyager 1 was in the magnetosphere are labeled MSP. From top to bottom are shown the radial speed, total proton density, ratio of the hot density component to the total density, hot and cold proton temperatures, ratio of hot to cold proton temperature, and magnitude of the magnetic field.

turns more radial than predicted. These regions are shaded and correspond to times when flow is over high magnetic latitudes. These signatures are those expected for a passage into the plasma mantle, a slow mode expansion fan which begins at the reconnection point on the dawn side (Zhang et al., 1990). The plasma in the mantle is a combination of solar wind and magnetosheath plasma. The mantle should expand away from the magnetopause into the magnetosphere and magnetosheath as it moves down the tail. This observation at Neptune was the first of the plasma mantle expanding into the magnetosheath region.

5. Waves in the magnetosheath

The waves observed in the outer planet magnetosheaths are generally similar to those at Earth, with one notable exception. Temperature anisotropies in the magnetosheath tend to be large, with $T_{\text{perp}} > T_{\text{par}}$, which can result in the generation of mirror mode waves. These waves are observed at Earth and are associated with lion roars (Tsurutani et al., 1982) and have also been reported at Jupiter and Saturn (Balogh et al., 1992; Tsurutani et al., 1992, 1993; Violante et al., 1995; Bavassano-Cattaneo et al., 1998). They sometimes exhibit magnetic peaks and dips, but also manifest as
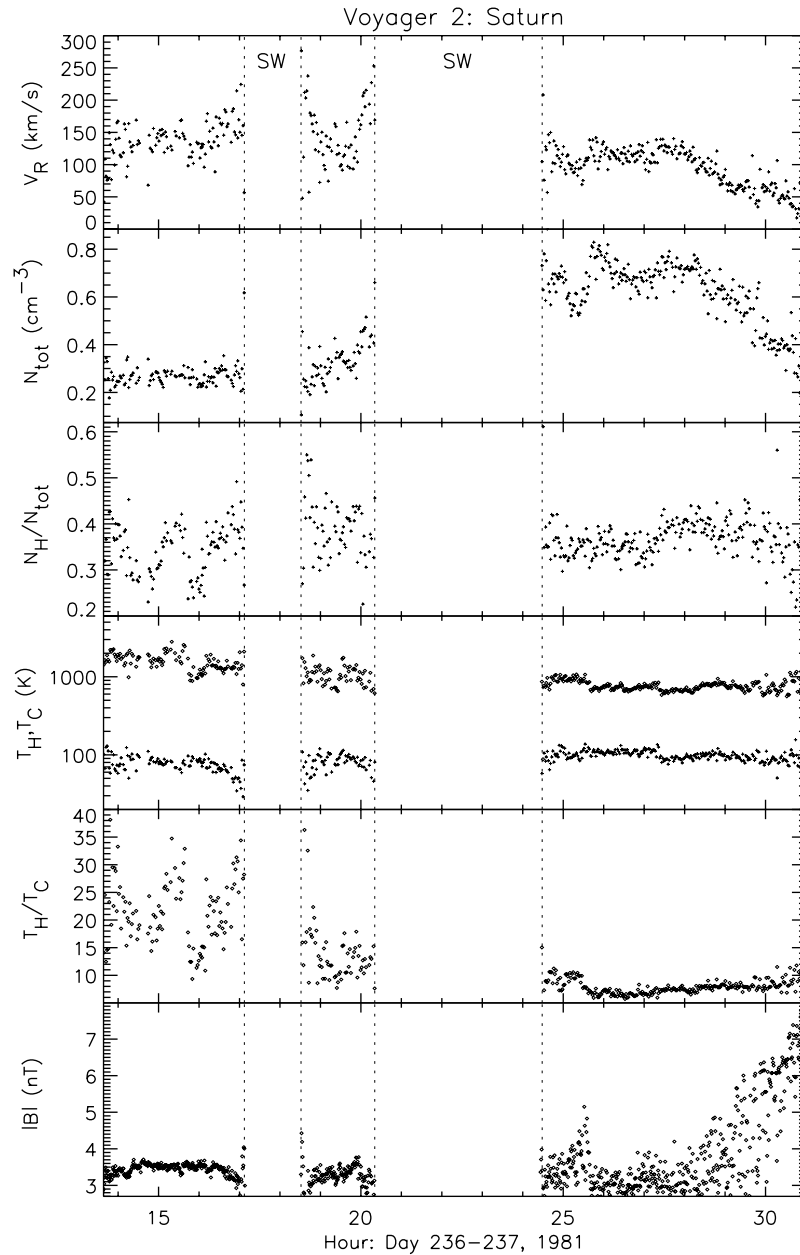
Fig. 7. The inbound magnetosheath data from Voyager 2 at Saturn. Periods where Voyager 1 was in the solar wind are labeled SW. From top to bottom are shown the radial speed, total proton density, ratio of the hot density component to the total density, hot and cold proton temperatures, ratio of hot to cold proton temperature, and magnitude of the magnetic field.

a series of magnetic holes (Winterhalter et al., 1994; Erdos and Balogh, 1996) as predicted by the non-linear model of mirror mode instability of Kivelson and Southwood (1996). Voyager's traversals of Saturn's subsolar magnetosheath provided an excellent opportunity to study the evolution of these waves from the bow shock to the magnetopause in quasi-stationary conditions. These waves are readily apparent as oscillations of the magnetic field magnitude in Figs. 6 and 7. Bavassano-Cattaneo et al. (1998) show that the mirror modes initially consist of a series of periodic oscillations whose amplitude increases and frequency decreases with time. Closer to the magnetopause, these waves evolve into

non-periodic, broad, large-amplitude structures with both field enhancements and rarefactions. Finally, in the PDL region within 1 h of the magnetopause, only narrow magnetic holes are observed. The fluctuations are compressive everywhere. The amplitude growth ($\Delta B/B$) downstream of the shock suggests the waves are generated near the shock and grow while being convected downstream. In the PDL, the plasma β is lower, about 1, so the plasma no longer supports the growth of mirror mode waves. Thus, these waves decay, leaving only relatively stable magnetic holes.

Waves on the magnetopause boundaries of Saturn and Uranus are reported based on multiple magnetopause
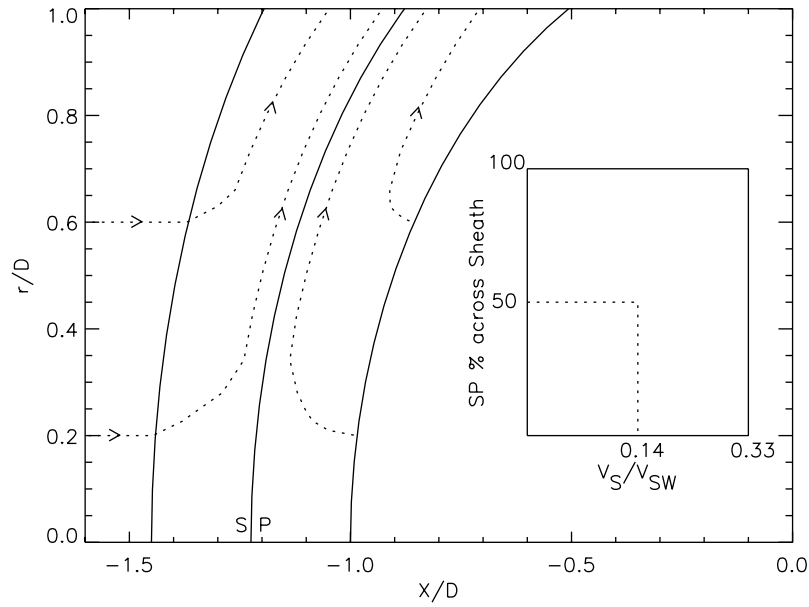
Fig. 8. Sketch of streamlines for a case when the magnetosheath region is expanding sunward. The axes are normalized by the magnetopause standoff distance. A new stagnation point (SP) forms in the magnetosheath. The inset graph shows the location of the stagnation point within the magnetosheath as a function of the ratio of the expansion speed (V_S) of the magnetopause to the solar wind speed (V_{SW}) (from Siscoe et al., 1980).
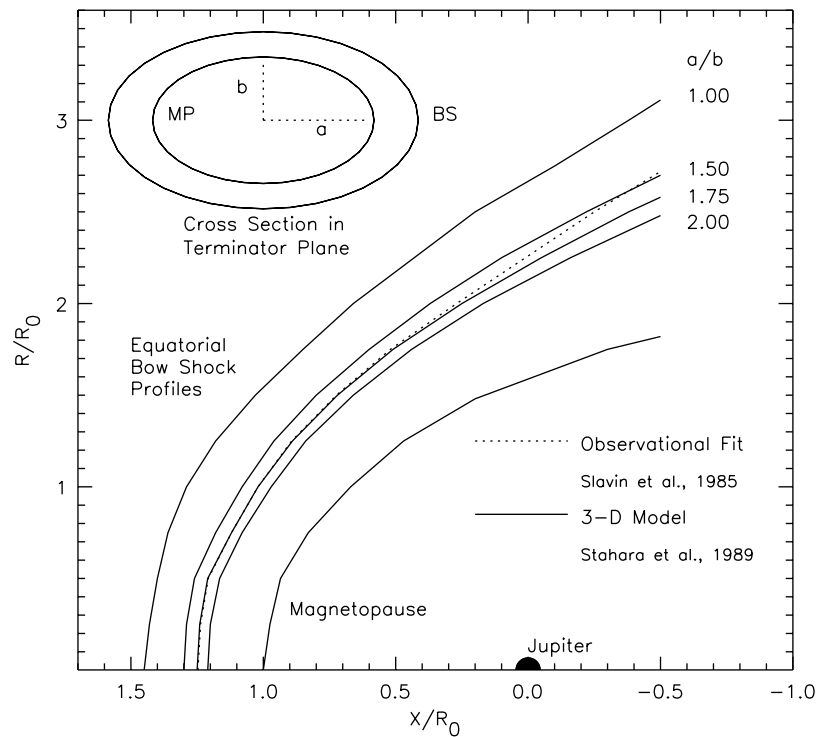

Fig. 9. Comparison of bow shock locations observed by Voyagers 1 and 2 at Jupiter with locations predicted by gasdynamic theory for various ratios of the magnetosphere major/minor axis (from Stahara et al., 1989).
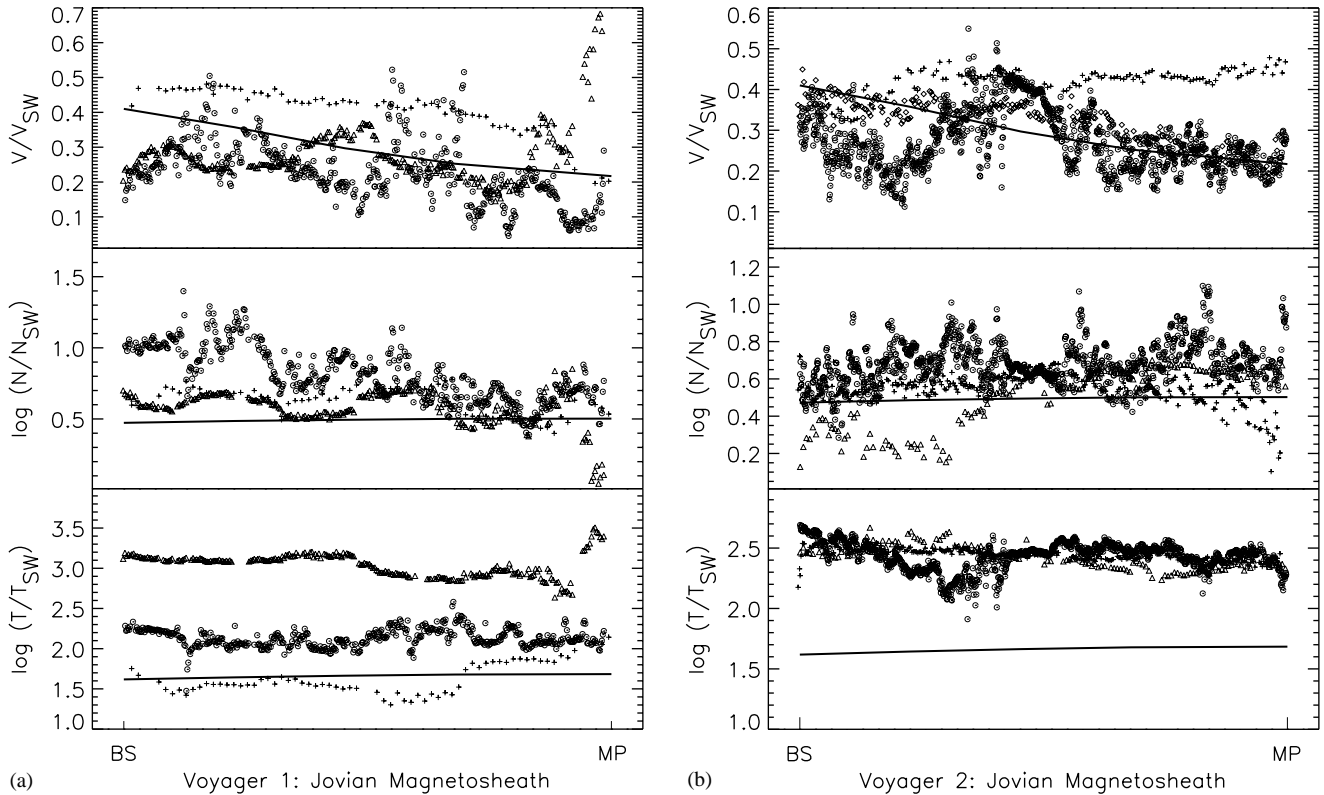
Fig. 10. Comparison of the speed, density, and temperature observed during the crossings of the Jovian magnetosheath by (a) Voyager 1 and (b) Voyager 2 with the predictions of the gas dynamic model of Stahara et al. (1989). The passes through the magnetosheath are normalized to the same time scale and to the solar wind conditions upstream of the bow shock for each pass. Model predictions are shown by the solid lines.

crossings. Lepping et al. (1981) interpret five magnetopause crossings observed by Voyager 1 inbound at Saturn as surface waves on the magnetopause. Their analysis shows that the normals of the magnetopause at the crossings are consistent with wave propagation along the magnetopause, not large-scale magnetopause motions which would result from changing solar wind dynamic pressure. A similar situation occurred at Uranus, where Lepping et al. (1987) showed that eight partial crossings of the magnetopause in the subsolar region had signatures consistent with surface waves on this boundary. Comparison of waves observed on the magnetopauses of Earth, Saturn, and Uranus shows wave speeds of 340, 180, and 76 km/s, amplitudes of 2×10^3, 26×10^3, and 4.5×10^3 km, and wavelengths of periods of 3, 23, and 7 min, respectively. Although the waves at Earth were observed at dawn and may not be directly comparable, speeds seem to decrease with distance from the Sun and the amplitudes and periods of the waves scale with obstacle size. Lepping et al. (1981) also propose that fluctuations in the field magnitude observed by Voyager 1 inbound may be driven by the magnetopause motion. The amplitude of these waves increases up to the magnetopause, but the density change is out-of-phase with the magnetic field magnitude change, so Lepping et al. (1981) interpreted these as slow-mode waves. It seems more likely that move-

ment of the magnetopause would compress both plasma and field; the fluctuations seen by Voyager 1 may be another manifestation of the mirror mode waves which have time to grow in the lower speed region near the stagnation point.

A class of waves/oscillations so far not observed at any other planet was observed in the outbound Uranian magnetosheath (Richardson et al., 1990). An example of these oscillations is shown in Fig. 13. They are characterized by factor of 4–10 changes in the plasma temperature and density which are anti-correlated. Large changes in the flow direction are observed, with the tangential velocity (in the RTN system; the Voyager trajectory passes through the dawnside ($T > 0$)) also anticorrelated with the changes in density. The magnetic field in these regions shows large, rapid variations with frequencies much larger than those of the plasma oscillations. Typical plasma parameters in this region are $\beta = 5$–10, $M_{MS} = 8$, proton gyrofrequency $= 0.04$ Hz, and Larmor radius $= 2000$ km. These oscillations are centered on times when Voyager 2 would be downstream a parallel bow shock and also occur when Voyager 2 is near the bow shock. The best hypothesis seems to be that these oscillations are downstream remnants of a parallel shock interaction although no quantitative modeling has been done.
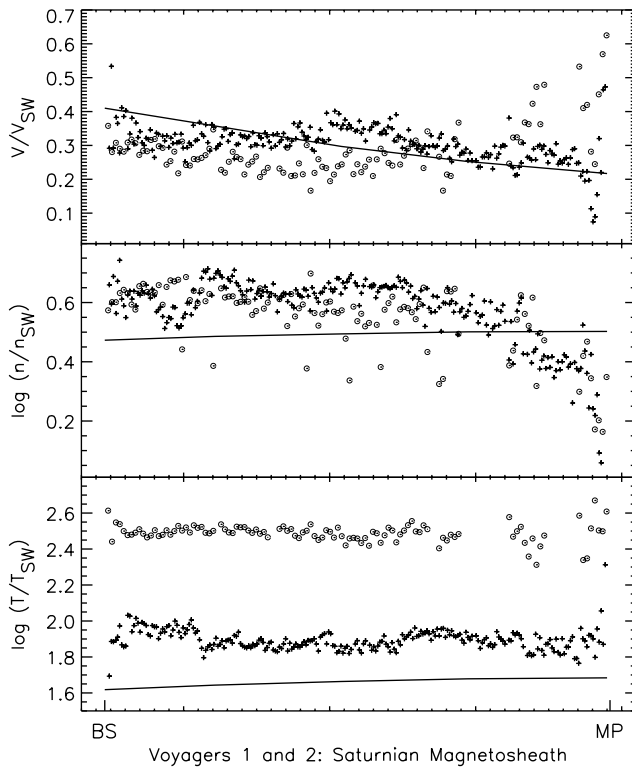
Fig. 11. Comparison of the speed, density, and temperature observed during the crossings of the Saturnian magnetosheath with the predictions of the Jovian gas dynamic model of Stahara et al. (1989). The passes through the magnetosheath are normalized to the same time scale and to the solar wind conditions upstream of the bow shock for each pass. Model predictions are shown by the solid lines.
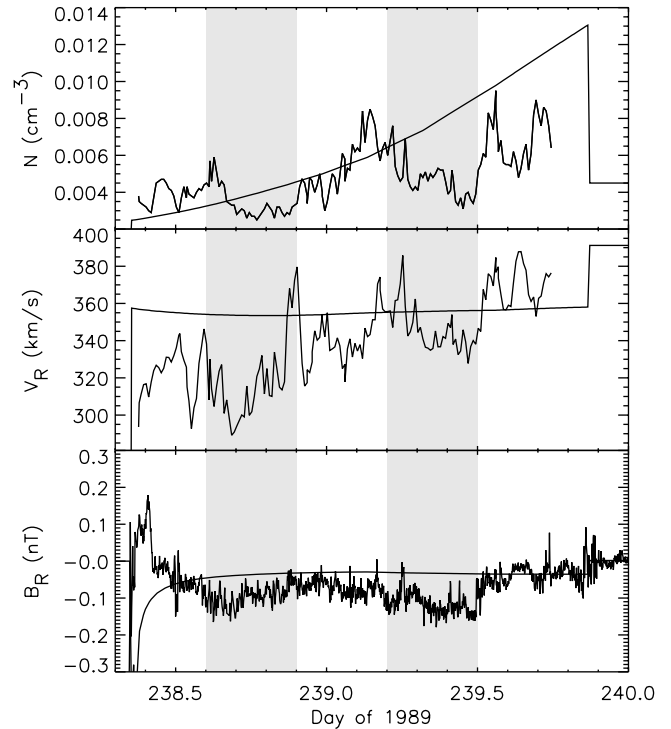

Fig. 12. Comparison of the magnetic field and plasma data observed in Neptune's magnetosheath downstream of the planet with that predicted by a gas dynamic model (solid line). The magnetopause and bow shock positions are labeled. The shaded regions show possible signatures of the plasma mantle.

6. Summary

The magnetosheaths of the outer planets provide a rich and varied environment for studying the interaction of the solar wind with varied magnetospheres. A major difference between these magnetosheaths and that of Earth are the ion distributions. At Earth ion distributions are generally well represented by Maxwellians with hot tails contributing on the order of 10% of the density. At Jupiter, Saturn, and Neptune, however, the distributions are comprised of two proton Maxwellian distributions with different temperatures. The ratio of the hot to total density averages about 40% and the hot to cold temperature ratio averages about 6–8. The shocks in the higher Mach number and more tenuous wind further from the Sun clearly maintain energy conservation by reflecting a larger percentage of ions at their first shock encounter so that they receive a double dose of heating. At Uranus distributions are more like Earth; more study is needed to understand the physics creating these ion distributions.

The magnetospheres of the outer planets are much larger and respond more dramatically to solar wind changes, particularly Jupiter. Thus time-dependent effects are very apparent in passages through these magnetosheaths. At Jupiter,
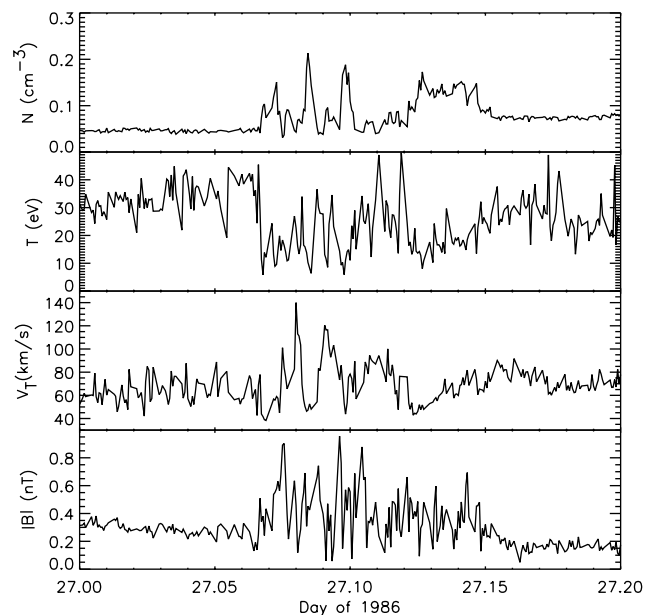

Fig. 13. An example of a wave mode so far unique to Uranus. The density is anticorrelated with the temperature and the tangential component of the magnetic field. The magnetic field exhibits large fluctuations in magnitude and direction.

outward motion of the magnetosphere due to solar wind pressure decreases results in large sunward magnetosheath flows. The importance of time-dependent effects makes direct comparison with gas dynamic predictions difficult; the general shape of the plasma profiles is similar to that predicted by gas dynamic theory with a few exceptions. One of these is the PDL, a non-gas dynamic effect observed near the magnetopause. Another is the first observation of the plasma mantle into the magnetosheath, observed by Voyager 2 at Neptune and identified in part by the departure of the observations from the gas dynamic theory. Another success of gas dynamic theory was the determination of the magnetopause shape; fits to observations of magnetopause and bow shock locations could only be obtained if the Jovian and Saturnian magnetospheres were significantly flattened at the poles.

Waves observed in the outer planet magnetosheaths are in most cases similar to those at Earth, but the low density, low magnetic field conditions make distance scales much longer and the waves easier to study. The Saturnian encounter was ideal for study of the evolution of mirror modes from the growth phase in the outer magnetosheath to decay in the PDL. One new wave mode in the Uranian magnetosheath has density anticorrelated with temperature and tangential speed and may be associated with regions downstream of parallel shocks.

The comparison of observations from other planets is an ideal way to test the physics we think we have learned from observations and models of Earth. The data sets so far obtained are only beginning to be mined. The sampling of topics shown here wets the appetite for what more detailed study and comparison of these magnetosheaths could teach us.

Acknowledgements

References

Balogh, A., Dougherty, M.K., Forsyth, R.J., Southwood, D.J., Smith, E.J., Tsurutani, B.T., Murphy, N., Burton, M.E., 1992. Magnetic field observations during the Ulysses flyby of Jupiter. Science 257, 1515–1518.

Bavassano-Cattaneo, M.B., Basile, C., Moreno, G., Richardson, J.D., 1998. Evolution of mirror structures in the magnetosheath of Saturn from the bow shock to the magnetopause. J. Geophys. Res. 103, 11,961–11,972.

Bridge, H.S., Belcher, J.W., Butler, R.J., Lazarus, A.J., Mavretic, A.M., Sullivan, J.D., Siscoe, G.L., Vasyliunas, V.M., 1977. The plasma experiment on the 1977 Voyager mission. Space Sci. Rev. 21, 259–287.

Erdos, G., Balogh, A., 1996. Statistical properties of mirror mode structures observed by Ulysses in the magnetosheath of Jupiter. J. Geophys. Res. 101, 1.

Fuselier, S.A., Schmidt, W.K.H., 1994. H^+ and He^{2+} heating at the Earth's bow shock. J. Geophys. Res. 99, 11,539–11,546.

Howe Jr., H.C., 1970. Pioneer 6 plasma measurements in the magnetosheath. J. Geophys. Res. 75, 2429–2437.

Hundhausen, A.J., Bame, S.J., Asbridge, J.R., 1969. Plasma flow pattern in the Earth's magnetosheath. J. Geophys. Res. 74, 2799–2806.

Kivelson, M.G., Southwood, D.J., 1996. Mirror instability, 2, the mechanism of nonlinear saturation. J. Geophys. Res. 101, 17,365.

Lepping, R.P., Burlaga, L.F., Klein, L.W., 1981. Surface waves on Saturn's magnetopause. Nature 292, 750–753.

Lepping, R.P., Burlaga, L.F., Klein, L.W., 1987. Surface waves on Uranus' magnetopause. J. Geophys. Res. 92, 15,347–15,353.

Mihalov, J.D., Wolfe, J.H., Frank, L.A., 1976. Survey for non-Maxwellian plasma in Jupiter's magnetosheath. J. Geophys. Res. 81, 3412–3416.

Montgomery, M.D., Asbridge, J.R., Bame, S.J., 1970. Vela 4 plasma observations near the Earth's bow shock. J. Geophys. Res. 75, 1217–1231.

Peterson, W.K., Shelley, E.G., Sharp, R.D., Johnson, R.G., Geiss, J., Rosenbauer, H., 1979. H^+ and He^{++} in the dawnside magnetosheath. Geophys. Res. Lett. 6, 667–670.

Phillips, J.L., Bame, S.J., Thomsen, M.F., Goldstein, B.E., Smith, E.J., 1993. Ulysses plasma observations in the Jovian magnetosheath. J. Geophys. Res. 98, 21,189–21,202.

Richardson, J.D., 1987. Ion distribution functions in the dayside magnetosheaths of Jupiter and Saturn. J. Geophys. Res. 92, 6133–6140.

Richardson, J.D., Zhang, M., Belcher, J.W., Siscoe, G.L., 1990. Plasma oscillations in the magnetosheath downstream from Uranus. J. Geophys. Res. 95, 6413–6421.

Richardson, J.D., Siscoe, G.L., Stahara, S.S., Spreiter, J.R., Szabo, A., 1994. The magnetosheath of Neptune: models and observations J. Geophys. Res. 99, 14,789–14,798.

Richardson, J.D., Paularena, K.I., Lazarus, A.J., Belcher, J.W., 1995. Radial evolution of the solar wind from IMP 8 to Voyager 2. Geophys. Res. Lett. 22, 325–328.

Sanders, G.D., Hills, H.K., Freeman, J.W., 1978. Two temperature structure of the magnetosheath at lunar distance (abstract). Eos Trans. AGU 59, 364.

Sanders, G.D., Freeman, J.W., Maher, L.J., 1981. A two-temperature plasma distribution in the magnetosheath at lunar distances. J. Geophys. Res. 86, 2475–2479.

Sckopke, N., Paschmann, G., Bame, S.J., Gosling, J.T., Russell, C.T., 1983. Evolution of ion distributions across the nearly perpendicular bow shock: specularly and nonspecularly reflected-gyrating ions. J. Geophys. Res. 88, 6121–6136.

Siscoe, G.L., Crooker, N.U., Belcher, J.W., 1980. Sunward flow in Jupiter's magnetosheath. Geophys. Res. Lett. 7, 25–28.

Slavin, J.A., Smith, E.J., Spreiter, J.R., Stahara, S.S., 1985. Solar wind flow around the outer planets: Gas dynamic modeling of the Jupiter and Saturn bow shocks. J. Geophys. Res. 90, 6275–6286.

Spreiter, J.R., Stahara, S.S., 1994. Gas dynamic and magnetohydrodynamic modeling of the magnetosheath: a tutorial. Adv. Space. Res. 14, 5–19.

Stahara, S.S., Rachiele, R.R., Spreiter, J.R., Slavin, J.A., 1989. A three dimensional gasdynamic model for solar wind flow past nonaxisymmetric magnetospheres: application to Jupiter and Saturn. J. Geophys. Res. 94, 13,353–13,365.

Szabo, A., Lepping, R.P., 1995. Neptune inbound bow shock. J. Geophys. Res. 100, 1723–1730.

Tsurutani, B.T., Smith, E.J., Anderson, R.R., Ogilvie, K.W., Scudder, J.D., Baker, D.N., Bame, S.J., 1982. Lion roars and nonoscillatory drift mirror waves in the magnetosheath. J. Geophys. Res. 87, 6060.

Tsurutani, B.T., Southwood, D.J., Smith, E.J., Balogh, A., 1992. Nonlinear magnetosonic waves and mirror mode structures in the March 1991 Ulysses interplanetary event. Geophys. Res. Lett. 19, 1267.

Tsurutani, B.T., Southwood, D.J., Smith, E.J., Balogh, A., 1993. A survey of low-frequency waves at Jupiter: the Ulysses encounter. J. Geophys. Res. 98, 21,203.

Violante, L., Bavassano-Cattaneo, M.B., Moreno, G., Richardson, J.D., 1995. Observations of mirror waves upstream of Saturn's magnetosphere. J. Geophys. Res. 100, 12,047–12,055.

Winterhalter, D.M., Neugebauer, D.M., Goldstein, B.E., Smith, E.J., Bame, S.J., Balogh, A., 1994. Ulysses field and plasma observations of magnetic holes in the solar wind and their relation to mirror-mode structures. J. Geophys. Res. 99, 23,371.

Wolfe, J.H., McKibben, D.D., 1968. Pioneer 6 observations of a steady state magnetosheath. Planet. Space Sci. 16, 953–969.

Zastenker, G.N., Avanov, L.A., Borodkova, N.L., Yukhnevich, Yu., 1994. Plasma dynamics in the magnetosheath. 1. Behavior of the main ion components. Cosmic Res. 31, 421–432 (translated from Kos. Issle. 31, 87–100, 1993).

Zhang, M., et al., 1990. Evidence for a diurnally rocking plasma mantle at Neptune. Geophys. Res. Lett. 17, 2285–2288.

Zwan, B.J., Wolf, R.A., 1976. Depletion of solar wind plasma near a planetary boundary. J. Geophys. Res. 81, 1636–1648.